Surface Debris Characterization and Mitigation Strategies and Their Impact on the Operation of River Energy Conversion Devices on the Tanana River at Nenana, Alaska

Prepared by

J. B. Johnson, J. L. Kasper, J. Schmid, P. Duvoy, A. Kulchitsky, M. Mueller-Stoffels, N. Konefal, A. C. Seitz

Alaska Center for Energy and Power,
Alaska Hydrokinetic Energy Research Center
Final Report June 2015

ACEP
Alaska Center for Energy and Power

UAF
UNIVERSITY OF ALASKA FAIRBANKS

Cover photo – Test barge with the Oceana turbine on deck behind the instrument tent, tethered behind the research debris diversion platform on the Tanana River, Alaska. A large debris object floats downstream nearby. (Photo taken by the Video Debris Observation System)

Table of Contents

List of Figures

List of Tables

Executive Summary

The research debris diversion platform (RDDP) has proven a robust platform for protecting surface-mounted river energy converters (RECs) from floating debris. With funding from the Alaska Energy Authority (AEA), grant ADN #R1416 "Debris Characterization and Mitigation," the design of the RDDP, as well as our ability to detect and understand its use with RECs, was significantly improved. In addition, the support of the AEA has enabled the development of new analysis techniques and technologies for describing and quantifying debris and its effect on RECs in Alaska's environments. Work on this project was divided into tasks as follows: (1) improvements to the RDDP and debris impact characterization, (2) the hydrodynamic impact of the RDDP, (3) video observations of debris, and (4) sonar debris monitoring. Though beyond the scope of the original project, an existing discrete element method (DEM) model, COUPi, was tested for simulating the interaction of debris with hydrokinetic infrastructure. A description of this DEM work is included here as a fifth task.

Task 1: Improvements to the RDDP and debris impact characterization. Tests and analyses of debris impacts on the RDDP indicate that the platform's ability to divert and clear debris improves significantly when all surfaces that come into contact with debris are covered with low-friction material, such as high-density plastic. The RDDP profile in the water is improved by properly ballasting the platform to counterbalance the downward drag at the front of the RDDP caused by water displaced under the debris sweep. The RDDP and mooring buoy system demonstrated the capability of withstanding significant debris impact during long-term deployments. In August 2013, the RDDP cleared debris after three large-scale impacts of up to 29 kN (6,600 lbf), with some debris taking more than 6 hours to clear. Interpretation of load cell data indicates that the debris impacting the infrastructure in the Tanana River likely consists of a mix of single and multiple debris objects. The RDDP will be redeployed during summer 2015 to protect two RECs: in July, the Oceana turbine operating behind the RDDP, and in August, a 5 kW NewEnergy turbine operated by the University of Alaska Fairbanks as part of the ALFA project funded by the U.S. Department of Energy (U.S. DOE).

Task 2: Hydrodynamic impact of the RDDP. A method for analyzing cross-river acoustic Doppler current profiler (ADCP) transects was developed to (1) maximize information derived from such standard, widely used ADCP measurements, and (2) enable the analysis of large-scale turbulence to determine its effects on REC performance. River velocity measurements performed during summer 2013 at the Tanana River test site (TRTS) were rotated into along- and cross-stream directions and projected onto an ideal straight transect. An optimal interpolation procedure was applied by means of MATLAB routines developed for the project that allowed interpolation of irregularly spaced measurements onto an equally spaced grid. From these gridded transects, averages and deviations from the average were calculated to characterize turbulence velocity fluctuations. The gridding analysis showed very little influence on the mean flow field (or on the vorticity) due to the presence of the RDDP, though questions about smaller-scale turbulence remain and measurement and analysis techniques need improvement. A short series of ADCP and acoustic Doppler velocimeter (ADV) measurements were made on the last day of the 2014 Oceana turbine deployment to determine the influence of the RDDP on REC performance. These measurements demonstrated that power output behind the RDDP is reduced and that the influence of the RDDP decreases with increasing distance from it. As no statistically

significant difference was found between the mean velocity at hub height at three distances behind the RDDP, we concluded that the reduction in power output is most likely due to the effect of the RDDP on small-scale turbulence.

Task 3: Video observations of debris. Significant improvements were made to the video debris observation system (VDOS). The VDOS is now able to record images of the river and floating debris at one frame per second, both from shore and from the RDDP. The imagery is then used to determine the size, location, and amount of surface debris in the river and to observe the interaction between debris and the RDDP. The VDOS was first built and tested in a breadboard configuration (i.e., a lab setting), and subsequently, a long-term performance test at the TRTS was completed in conjunction with the Oceana turbine deployment. Presently, the VDOS is capable of long-term autonomous operation and thus is a suitable tool for use in remote locations where hydrokinetic projects are being considered.

Task 4: Sonar debris monitoring. The preliminary investigation of whether a BlueView sonar "camera" is suitable for detecting debris was largely unsuccessful because we were unable to obtain long-term observations with the system. In 2013, BlueView's operating software continually "hung up" during multiple daylong deployments. Additionally, it was determined that the AHERC BlueView system is unable to detect debris beyond ~15 m due to signal scattering by the sediment carried in the Tanana River. Discussions with Teleydyne BlueView indicate that the company has a lower-frequency (450 kHz) sonar that may perform better in this heavily silted river than higher-frequency sonars, such as the one AHERC currently possesses. Teledyne BlueView indicated an interest in working with AHERC to solve the resolution and software reliability issues. The most recent versions of the Teledyne BlueView operating software appear to address past reliability issues, though these remain to be field tested. A split-beam sonar owned by the University of Alaska Fairbanks, deployed in September 2014for fisheries monitoring in support of the Oceana turbine, repeatedly operated for periods of up to a full day unattended using only a small Honda generator as a power source. With funding from the U.S. DOE, a power and data system has since been developed for long-term operation of the BlueView and split-beam sonar systems.

Task 5: COUPi DEM modeling. In addition to the four tasks that comprise the core of the project, the capability and techniques for simulating debris interactions with hydrokinetic infrastructure such as the RDDP were developed as a complement to the four core tasks. The COUPi DEM was used for simulating the impact of debris on the RDDP to provide a qualitative way of examining the process of debris interaction with the platform and its debris sweep. Simulations indicate that the ability of the RDDP to clear debris is influenced by the shape of the debris object and the contact friction between debris and the platform. With funding from the U.S. DOE ALFA project, the COUPi DEM simulations will be improved by adding more realistic buoyancy effects and RDDP features, including a rotating debris sweep and a variable opening angle between the platform's pontoons.

Overall, the RDDP and buoy system, developed as part of prior work directed by Alaska Power and Telephone and refined under this project, has proven a strong platform for protecting surface-mounted RECs from floating debris. Despite progress, however, many questions about subsurface debris remain, including its potential to disrupt subsurface RECs. The question of how best to bring hydrokinetic power to shore in debris-infested river waters

remains largely unexplored. While we have made substantial progress in maximizing the utility of ADCPs for making hydrodynamic measurements relevant to REC installations, shortcomings in the current generation of ADV mounts require a greater investment of time so that smaller-scale turbulence and its effect on REC power output can be better understood. While the RDDP/buoy/pontoon barge protection scheme, developed partly with funding from the AEA, has proven successful, cost-effective installations of RECs in remote communities will require refinements in REC+debris protection systems to achieve affordable and practical implementations. The tools developed during this study are a step forward in our ability to evaluate any future hydrokinetic projects, both within and outside Alaska. As additional steps are taken toward employing hydrokinetic energy systems in Alaska's waterways, we must consider the effects of any new hydrokinetic infrastructure on habitat, including that of the state's fisheries.

Finally, given the short open-water season in Alaska, the economics of hydrokinetic energy must be determined, including a realistic projection of the levelized cost of energy for hydrokinetic energy systems. Remaining issues require systematic development of new platforms (e.g., improved ADV mounts or simpler, lighter, and stronger debris-mitigation schemes integral to REC systems) and techniques (e.g., improved understanding of the limits of sonar for fisheries monitoring in turbid rivers that carry large amounts of woody debris). Such efforts require continuing cooperation between state and federal agencies, the university, and the private sector.

Introduction

In 2010, three different efforts to demonstrate river energy converters (RECs) deployed from floating platforms (two in Alaska and one in Canada) were ended because of problems with woody debris (Johnson and Pride 2010; Tyler 2011; NUL 2012; Johnson et al. 2013). Alaska Power and Telephone's (AP&T's) 2010 demonstration of a 25 kW New Energy Corp. EnCurrent REC in the Yukon River at Eagle, Alaska, worked well until problems with both floating and submerged debris caused AP&T to end the demonstration. Debris on the river's surface that piled up in front of AP&T's floating platform posed a major hazard to operations and to personnel safety, and subsurface debris collected on underwater power and anchoring cables.

Because of difficulties with operating their REC at Eagle, AP&T decided to abandon plans for deploying the REC in 2011. The company initiated a project with the Alaska Hydrokinetic Energy Research Center (AHERC) to examine ways to reduce the hazard of surface debris for REC devices deployed from floating platforms. During this study, AHERC developed a surface research debris diversion platform (RDDP) to investigate the important factors associated with diverting surface debris around REC devices. The RDDP consists of two pontoons connected at their upstream end by hinged pins that allow adjustment of the separation angle between the pontoons using a hydraulic pump. A debris sweep, consisting of a cylinder that is free to rotate in clockwise or counterclockwise directions, was placed in front of the pontoons to prevent debris from catching on the front of the RDDP. The debris sweep's rotation depends on the torque from impacting debris acting on the debris sweep (Johnson et al. 2014).

Tests and analyses of the RDDP's ability to divert debris demonstrated the debris sweep's effectiveness at preventing debris from collecting on the front of the platform. The tests also indicated that the efficiency of the RDDP to shed debris depends on the friction between debris and the pontoons and debris sweep, the inertia of the debris sweep, the opening angle of the pontoons, and the pontoons' draft. Other factors that were found to affect RDDP performance included the aspect ratio of a debris object's diameter divided by its length (higher aspect ratios result in increased debris pinning forces), and the river current velocity (higher current velocities increase debris-clearing forces.

The RDDP diverts debris from its original flow path to a flow path along the edge of the wake produced by the platform. Efforts to determine the magnitude of river current turbulence caused by the RDDP using acoustic Doppler current profiler (ADCP) measurements were inconclusive, as it was not possible to separate turbulence generated by the RDDP from turbulence that occurs naturally in the river.

In the following sections, we report on the results of a study sponsored by the Alaska Energy Authority (AEA) that builds on the project commissioned by AP&T to further characterize river surface debris and examine the performance of the RDDP. The AEA-sponsored study goals included conducting long-term deployments of the RDDP, determining the RDDP's effect on local river currents, developing a video debris observation system (VDOS) to monitor river surface debris, and examining the use of sonar to detect subsurface debris. Of particular interest were the magnitude of debris impact loads on the RDDP and improving the

RDDP's performance. Performance factors such as friction between the RDDP components and debris, debris sweep inertia, the pontoons' opening angle, and the RDDP/mooring buoy system are known to be important ones, affecting the platform's ability to reduce the problem of surface debris for REC devices. In addition to field-related work, we developed preliminary descriptions of debris impact with the RDDP using discrete element method (DEM) modeling. A benefit to the study was that AHERC conducted testing of an Oceana Energy Company turbine during 2015, enabling direct measurement of the effect of natural river turbulence and RDDP-generated turbulence on turbine performance.

Methods

RDDP Design and Testing

RDDP design modifications

Several design modifications to the RDDP to improve its performance, as identified by Johnson et al. (2014), include covering the pontoon surfaces with low-friction, high-density plastic (Figure 1), improving the load cell installation, and adding solid ballast at the back of the RDDP. Debris impact tests conducted during the AP&T study (Johnson et al. 2014) demonstrated that when the RDDP's steel pontoons had wide opening angles, debris could be pinned against the pontoons or caught on the upright members of the guardrails. The tests also demonstrated the value of covering the debris sweep with high-density plastic, thereby presenting a smooth surface to debris objects that would reduce contact friction between the debris sweep and the debris. As a result of these debris impact tests, a continuous sheet of plastic was used to cover the outer surfaces of the RDDP pontoons, and the guardrails were moved from the outside of the pontoons to the inside of the pontoons (Figure 1).

Figure 1. The RDDP debris sweep (front cylinder) and pontoons with plastic sheet covering to reduce contact friction between the RDDP and debris.

Deployment of the RDDP during periods of high river stage demonstrated that the platform tended to float with its debris sweep pitched down (Figure 2) due to the force of water against the debris sweep and to upwelling of water to the rear of the debris sweep. To counteract this problem, ballast plate mounts were installed on the inside surface at the rear of the pontoons (Figure 3), which provided a way to add ballast as necessary, supplementing the ballast by filling the pontoon baffle chambers with water.

Figure 2. RDDP with nose pitched forward due to high river velocity prior to installation of ballast plates.

Figure 3. RDDP ballast plates.

RDDP debris impact force measurements

The RDDP debris impact force measurements were made using a high-resolution load cell (2,000 lbf [9 kN]) connected in series, using a breakaway cable, with a low-resolution, high-capacity load cell (20,000 lbf [90kN]) (Figure 4). In this configuration, load readings from both high-resolution and low-resolution load cells can be made simultaneously, with the high-resolution load cell taken offline only when the breakaway cable fails as debris impact loads exceed about 9 kN. When this occurs, a slack cable connecting the 90 kN load cell to the shackle connection takes up the load that had been carried by the breakaway cable and 9 kN load cell.

In past iterations, the 9 kN and 90 kN load cells were connected in parallel, with the 9 kN load cell carrying the load and the 90 kN load cell attached to a slack line. When a debris impact caused the breakaway cable to fail, the load would transfer from the 9 kN load cell to the 90 kN load cell. As part of this project, the geometry of the shackle connection was modified to allow the 9 kN and 90 kN load cells to be placed in-line to provide a means of synchronizing any measurement offset between the two load cells while still preventing the high-resolution load cell from being damaged during extreme impact events.

Field activities for the RDDP during 2013 (Table1) began in late June with the recovery of the anchor chain and deployment of the mooring buoy. The mooring buoy deployment schedule is strongly dependent on Inland Barge's cargo delivery activities and on whether or not the nearshore riverbed has thawed. The RDDP was deployed at the Tanana River test site (TRTS) using AHERC's research Jon boat in early July to maximize the exposure time of the RDDP to debris impacts. The RDDP was removed from the TRTS in August to install a low-friction plastic sheet on the outer surfaces of the pontoons (Figure 1) and was redeployed in early September, with final retrieval for the season in October.

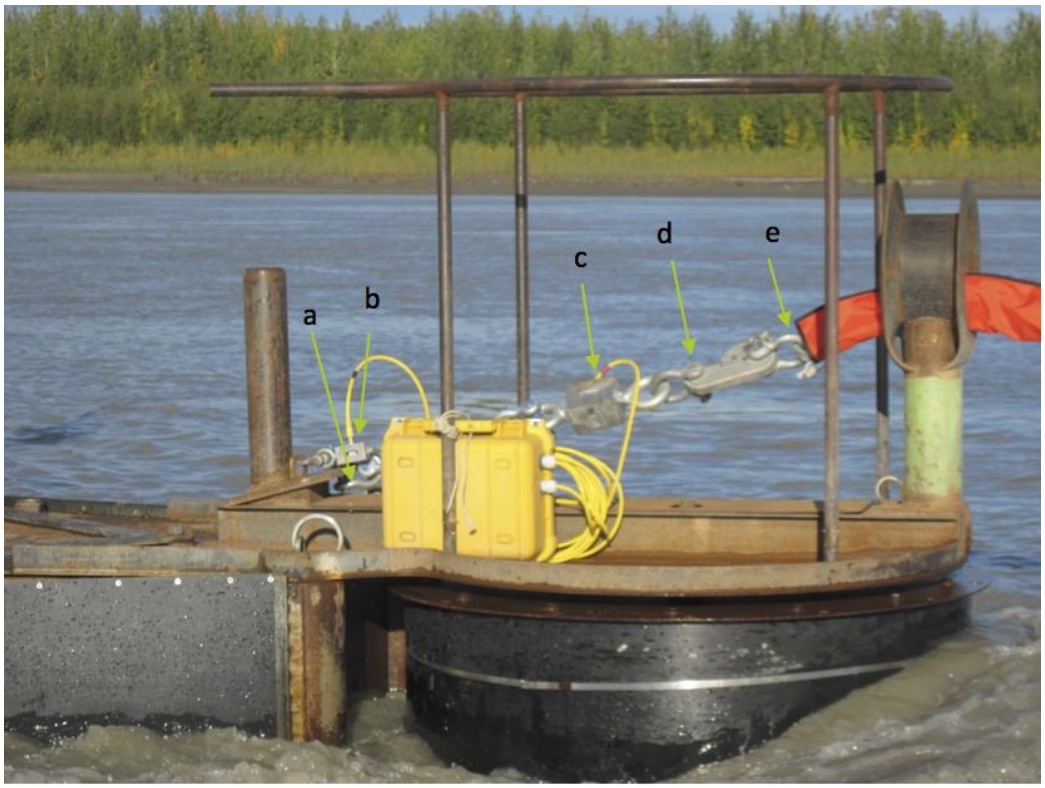

Figure 4. Load cell connection setup: (a) shackle connection to RDDP; (b) high-resolution load cell (2,000 lbf/9 kN); (c) high-capacity load cell (20,000 lbf/90 kN); (d) quick release mechanism; (e) connection to mooring tether line.

In September, a series of debris impact tests were conducted with the RDDP at its widest opening angle and with the pontoons covered with low-friction plastic. No debris objects became pinned to the RDDP pontoons in this test, as had occurred when the pontoon's steel surface was bare, providing further evidence of the value of using low-friction material on debris diversion devices.

Load cell measurements during 2014 started on August 1, in conjunction with readying the test site for the Oceana hydrokinetic turbine. On August 25, the first temporary attachment of the barge behind the RDDP took place. On September 5, the test barge was positioned behind the RDDP, and the truss used to support the Oceana turbine was tested with a dummy load prior to installation of the turbine. On September 9, the Oceana turbine was set up on the truss, and testing continued to late September. Due to relatively low water current velocity, very little debris was present in the river flow, and no debris collisions with the RDDP occurred.

Table 1. Project activities during 2013 and 2014.

RDDP deployment 2013	
6/6/2013	Conducted initial ADCP hydrodynamic/turbulence transects
6/24/2013	Deployed mooring buoy with help of Inland Barge
7/2/2013	Deployed RDDP in Tanana River
7/3/2013	Conducted ADCP hydrodynamic/turbulence transects and point turbulence measurements behind RDDP
7/4/2013	Conducted ADCP hydrodynamic/turbulence transects and point turbulence measurements behind RDDP
7/23/2013	Conducted ADCP hydrodynamic/turbulence transects
7/24/2013	Conducted BlueView imaging sonar subsurface debris observing test and ADCP hydrodynamic/turbulence transects
8/1/2013	Conducted ADCP hydrodynamic/turbulence transects
8/7/2013	Conducted ADCP hydrodynamic/turbulence transects
8/8/2013	Measured ADCP point turbulence behind RDDP; compared side-by-side BlueView/DIDSON imaging sonar with Alaska Department of Fish and Game; conducted single ADCP turbulence transect
8/8/2013	Removed RDDP from mooring for UHMW modification; add provision for additional steel ballast; modify mooring attachment to allow in-line connection of load cells
9/9/2013	Redeployed RDDP in river after modifications
9/25/2013	Positioned BlueView on fixed mount on the RDDP for test of long-term unattended deployment
10/1/2013	Removed RDDP from station for transport to Fairbanks
RDDP deployment 2014	
6/9/2014	Deployed mooring buoy with help of Inland Barge
6/15/2014	Installed river stage sensor
7/21/2014	Deployed RDDP in the Tanana River
7/28/2014	Installed long RDDP tether to increase distance between buoy and RDDP
8/5/2014	Adjusted RDDP ballast
8/18/2014	Installed Oceana truss on Murdock pontoon barge
8/25/2014	Deployed barge in the Tanana River
9/5/2014	Tested the barge+truss+hydraulic system with dummy weight to simulate Oceana turbine
9/11/2014	Lowered Oceana turbine into water from barge and place behind RDDP
9/11–22/2014	Tested with Oceana turbine
9/22/2014	Conducted AHERC/Oceana hydrodynamic measurements at different distances behind the RDDP
9/23/2014	Removed Oceana turbine from barge
9/23/2014	Removed RDDP from the Tanana
9/29/2014	Transported RDDP to Jon’s Machine Shop for off-season modifications
10/1/2014	Removed buoy from the Tanana River
10/7/2014	Removed barge from the Tanana River
10/8–10/2014	Disassembled barge for transport to Fairbanks

Hydrodynamic Measurements

The objective of the hydrodynamics measurement efforts is to characterize how the buoy, RDDP, barge, and turbines affect hydrodynamic conditions in rivers. To this end, in summer 2013 multiple cross-river ADCP sections were occupied at the TRTS to measure streamwise, cross-stream, and vertical velocities. Beginning above the buoy and ending downstream of the RDDP, cross-river sections were occupied at 20 m intervals. In the absence of regularly spaced data, it is not possible to calculate average sections, since each measurement is taken at a different location. Thus, in order to analyze the large volume of data produced by these and past years' measurements, as well as to maximize the information produced by each transect, a procedure for interpolating individual transects onto a regularly spaced grid of points was developed. Gridding the data in this manner enables the calculation of average velocities across a given river cross section and allows the calculation of velocity fluctuations in an individual transect from the mean transect. In other words, the turbulence velocities at a given grid point can be calculated. From this information, spatial and time domain descriptions of the turbulence can then be derived (i.e., the size and wavelength of the turbulence). Repeatedly measuring the velocity near the RDDP and then analyzing the data using the gridding procedure enable a detailed description of how the RDDP affects the hydrodynamics that develop. A manuscript for peer-reviewed publication describing the gridding procedure is in draft form.

In September 2014 during the Oceana turbine testing, a 1200 kHz Teledyne RD Instruments ADCP sampling at about 1 Hz (exact sample rate depends on the depth) and a Nortek acoustic Doppler velocimeter (ADV) sampling at 16 Hz were mounted on the bow of the barge. The ADCP data were subsequently analyzed using several techniques developed during the gridding procedure.

Findings are detailed in the Results and Discussion section, under subsections *Hydrodynamic Measurements* and *Oceana Turbine Testing and the Influence of River and RDDP-Generated Turbulence*.

Sonar Measurements of Subsurface Debris

During summer 2013, we tested AHERC's BlueView sonar "camera" for its effectiveness at identifying, characterizing, and tracking subsurface woody debris. The focus of this effort was on determining whether the BlueView system was suitable for use in an "active" debris mitigation strategy, detecting the presence of debris and then activating debris mitigation. The thought was that an active debris mitigation system would protect hydrokinetic infrastructure and, at the same time, maximize the energy extracted from river currents by minimizing the reduction in flow caused by passive debris mitigation devices such as the RDDP (i.e., barriers, permanently mounted upstream of a REC). As part of this evaluation, a side-by-side comparison of the capabilities of AHERC's BlueView sonar and a similar DIDSON system owned by the Alaska Department of Fish and Game was conducted (Table 1, 8/8/2013). We found that the systems were comparable in their capabilities.

Further testing of the BlueView camera indicated that, though the high-frequency system currently owned by AHERC is capable of imaging debris at short distances (<15 m), longer-range capabilities are necessary to allow for adequate response time in an active debris

mitigation system. To achieve longer ranges, a lower-frequency system is needed. The BlueView software available at the time of testing in 2013 proved incapable of operating unattended for periods exceeding several hours. In contrast, long-term tests with a UAF-owned split-beam sonar, used with the RDDP in place of the BlueView during the 2014 Oceana turbine deployment, indicated that the operating system for the UAF split-beam sonar is reliable enough for long-term unattended data collection. During the course of the project, we determined that software for automated identification of debris would require significant development.

To address these issues, AHERC initiated communication with the manufacturer, Teledyne BlueView. In February 2015, a follow-up round of lab testing of an upgraded version of the BlueView operating system indicated that it is more stable than previous versions and may be capable of sustained long-term operation. Field tests of the upgraded version will occur in July 2015 as part of required fisheries monitoring during deployment of the Oceana turbine and later in the summer during the U.S. DOE-funded ALFA project. Through the ALFA project, AHERC is funded to develop an autonomous sonar power and data collection system for tracking fish and subsurface debris using active sonar technologies including the BlueView and a split-beam sonar. Existing software packages will be tested for analysis of the sonar data during the ALFA project. Note that the robust power and sonar data-collection system is based in part on a similar system developed for the VDOS, as described in the following section.

Video Debris Observation System

We attempted to develop a video debris observation system (VDOS) in 2011 during the AP&T/Denali Commission study on debris mitigation. While some data were obtained, the VDOS worked only intermittently because of problems with the power system and freeze-up of the control computer. The power system consisted of a solar panel, batteries, and a manual-start generator that was used to charge the batteries when the site was visited. Web style cameras were used to observe debris. The experience gained in developing the prototype debris observation system demonstrated the need for improvements in the power generation system, video cameras, control system, and data recording components to achieve the reliability required for unattended operation in remote locations.

Figure 5. The shore-mounted VDOS system.

The current VDOS power generation system includes batteries, a solar panel, and an auto-start generator (Figure 5). The main components of the VDOS include two high-resolution cameras capable of recording images at one frame per second and a network attached storage (NAS) device for storing and processing image data.

Each component is controlled by a programmed relay and powered by 120 VAC or 24 VDC, depending on the component. The programmed relay enables self-monitoring of the system and replaces the control computer. That is, should a device on the internal network "hang up," the relay will sense this and reboot the component. Four 1TB drives are configured as two sets of mirrored drives (2, 1TBX1TB pairs) formed into a single array. This configuration allows for the loss of two drives without the loss of any data.

One camera is shore-mounted to observe surface debris and the RDDP's performance during debris impacts. A second camera is available to mount on the RDDP to observe debris approaching and interacting with the RDDP or to observe how well debris is diverted by the RDDP. Data from the RDDP-mounted camera is transmitted to the shore-based base station via a wireless communications link (Wi-Fi).

Using the 2014 VDOS data, we performed a manual count to analyze debris statistics. Data were collected from September 9 to September 16, 2014, and during the manual count, debris was counted for the first 5 minutes of every hour during daylight hours. Debris was then classified by size into three categories: small, medium, and large (Figure 6). Small debris was anything that could be removed from the river by hand and lifted over one's head. Medium-sized debris was anything that was too large to lift over one's head, but too small to have sufficient buoyancy to carry the weight of a person downriver. Large-sized debris was anything that was large enough to have sufficient buoyancy to support a person. Debris was also classified by location in the river looking downstream, with the river divided evenly into three segments: river left, river right, and mid channel. During the manual count, we observed no impacts with the debris diverter. River velocity was recorded at 1.68 m s^{-1} from the barge on September 22, 2014

An effort to develop an automated method of examining VDOS images to detect debris was unsuccessful, as the detection scheme had difficulty differentiating between debris objects and natural vortex eddies in the river. The method was successful at detecting debris, but reported many false positives due to the abundance of eddies in the river. Efforts to improve the automated detection system are ongoing.

Discrete Element Method Modeling Debris Impact on the RDDP

Simulating debris impacts against structures in a river is a challenging problem that involves a debris object moving in the current's flow at a velocity approximating that of the river. When debris objects impact a fixed structure such as the RDDP, the velocity of the debris objects will decrease dramatically, with a consequent transfer of momentum impulse to the structure that may result in large local forces at the point of impact. In addition to the complexity of momentum impulse applied to the RDDP, the effects of RDDP geometry, surface friction, properties of the debris object (mass, size, geometry, surface roughness), and turbulence in the flow affect the performance and survivability of the RDDP.

Figure 6. Woody debris objects. From top to bottom: large debris, medium debris, and scattered small and medium debris.

The discrete element method (DEM) can explicitly simulate the displacement, velocities, and forces of assemblies of objects. The DEM stores the shapes, velocities, and locations of the objects; finds contacts; calculates forces and moments at each contact due to particle contact physics; and calculates the movement of each particle within the aggregate (Cundall and Strack 1979; Hopkins 2004). Each component of debris impact with the RDDP is described as a separate object (e.g., the debris object, the RDDP debris sweep, each of the two RDDP pontoons). The RDDP objects are held fixed, while the debris objects are subjected to constant acceleration and drag.

As drag is a function of particle velocity, the debris object acceleration is eventually counterbalanced by drag to achieve a constant debris object velocity. Upon impact with the RDDP, the debris object decelerates to near zero velocity, transferring impulse momentum to the RDDP and a constant force that depends on the mass of the debris object and the applied

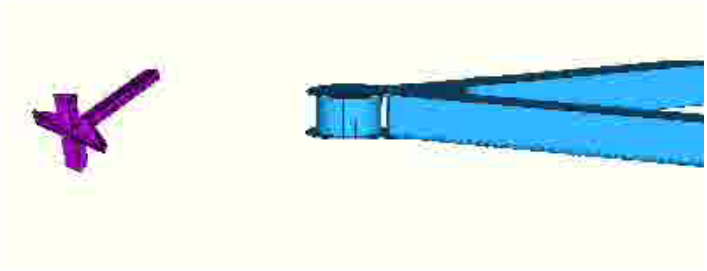

Figure 7. DEM simulation of a debris object moving toward the RDDP

acceleration function. We use the COUPi DEM to simulate debris impacts against the RDDP for two different shapes and three different contact friction values (Figure 7). The COUPi DEM was developed at the University of Alaska Fairbanks under the NASA Lunar Science Institute (NLSI) project "Scientific and exploration potential of the Lunar poles" to simulate mobility and excavation processes on the Moon, but it can readily be applied to a variety of complex problems. At present, our DEM simulations are qualitative, as we apply constant acceleration and drag to the debris object, rather than a realistic current velocity field, and no buoyancy term is in the simulation. Also, the RDDP debris sweep is not free to rotate, and the opening angle of the pontoons is not adjustable. These features are planned future additions to the simulation.

The primary information obtained from COUPi DEM simulations is the influence of the debris sweep and friction on the ability of the RDDP to divert debris. With an improved model, the effects of debris sweep inertia and pontoon opening angle on the RDDP's debris diversion capabilities may be described.

Oceana Turbine Performance Testing

During September 2014, performance tests of the Oceana Energy Company's hydrokinetic turbine were conducted at the Tanana River test site. The Oceana hydrokinetic turbine was deployed from AHERC's test barge that was moored immediately downstream from the RDDP, which was moored to a midstream buoy attached to an embedment anchor (Figure 8).

To better understand the potential influence of natural river turbulence and RDDP-generated turbulence on the power output of hydrokinetic devices, we operated the Oceana turbine at a distance of 14.5, 50, and 100 m downstream from the RDDP. The 14.5 m distance is the closest distance of the test barge when its bridle is moored directly to the RDDP spreader bar (Figure 9). This mooring arrangement provides maximum protection of the test barge from debris. When the bridle is tethered through a centering ring on the spreader bar, the barge is rigidly fixed to the RDDP. If the RDDP is hit by a large inertia debris object the combined inertia of the barge and RDDP reduces the rotation of the

Figure 8. AHERC test barge, with the Oceana hydrokinetic turbine on deck, moored behind the RDDP as a debris object floats by.

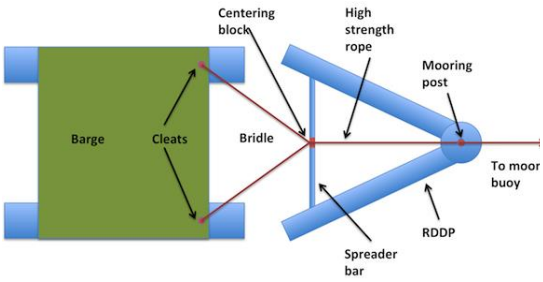

Figure 9. Mooring configuration of the test barge and RDDP.

RDDP/barge system about the RDDP's mooring post. If the debris object impacts with enough momentum to cause the RDDP to rotate around its mooring post, then the barge and RDDP rotate together such that the debris object clears the RDDP pontoon and barge.

The Oceana turbine operations at 50 and 100 m were used to assess how RDDP-generated turbulence dissipates with distance behind the RDDP. An abstract of this testing was presented at the annual Marine Energy Technology Symposium this past April (Johnson et al. 2015), and it is expected that a peer-reviewed conference proceeding will result from this work.

Results and Discussion

RDDP Design and Testing

The RDDP's primary modification was the addition of low-friction plastic sheeting on the outside surface of the pontoons. The plastic sheeting, which also covered the weld beads and geometry protrusions, reduced the contact friction between the RDDP and debris. This modification eliminated the problem of debris pinning against the RDDP pontoons due to river current forces and debris catching on weld beads and small protrusions at the rear of the RDDP. Test experience with the RDDP has demonstrated that debris readily adheres to rough surfaces, small protrusions, or sharp angles, and then collects additional debris.

All objects used during the debris impact tests conducted during 2013 on the RDDP, with its plastic-covered pontoons open to their maximum angle of 74 degrees, were diverted around the platform without becoming pinned to the pontoon surfaces. These test results indicate a marked improvement in the diversion capabilities of the RDDP when compared with results from diversion tests conducted in 2012 on steel pontoon surfaces, during which debris pinned against the RDDP, with the pontoons at an opening angle of 58 degrees.

The primary goal during deployment of the RDDP and mooring buoy system in 2013 was to expose it for as long a period as possible to natural river debris floating downriver. Long-term deployments took place from July 2 until August 8, when the RDDP was removed from the river to install plastic sheeting on its pontoons, and from September 9 until October 1, after the plastic sheeting had been attached to the pontoons. During both periods, the pontoons had an opening angle of 38 degrees (Figure 7).

Load cell measurements indicate that several relatively large impact events occurred during August 3 through August 5, and that a smaller impact event occurred on August 19 (Figures 10, 11, and 12). On August 2 at 9:55 a.m., a sudden impact occurred that parted the sacrificial link protecting the 9 kN load cell. The 9 kN cell reported a maximum load of 3.6 kN when the link broke. The 90 kN load cell then recorded a maximum load of 14 kN, with the load decreasing to background values within 1 minute. It is not possible to fully understand the nature of the impact event, as no video observations are available. It is

possible, however, to make reasonable interpretations that provide some indication of how the RDDP's interaction with the debris evolved. The first debris impact occurred August 3, 2013, at 4:11 p.m., with an increase in load to about 29.5 kN (6,600 lbf) over a period of 25 minutes, likely caused by the momentum of the debris. The load then decreased to 26 kN over a period of 75 minutes due to the force of current as the debris object remained in contact with the RDDP. The RDDP force then dropped to nearly pre-impact levels as the debris cleared the platform.

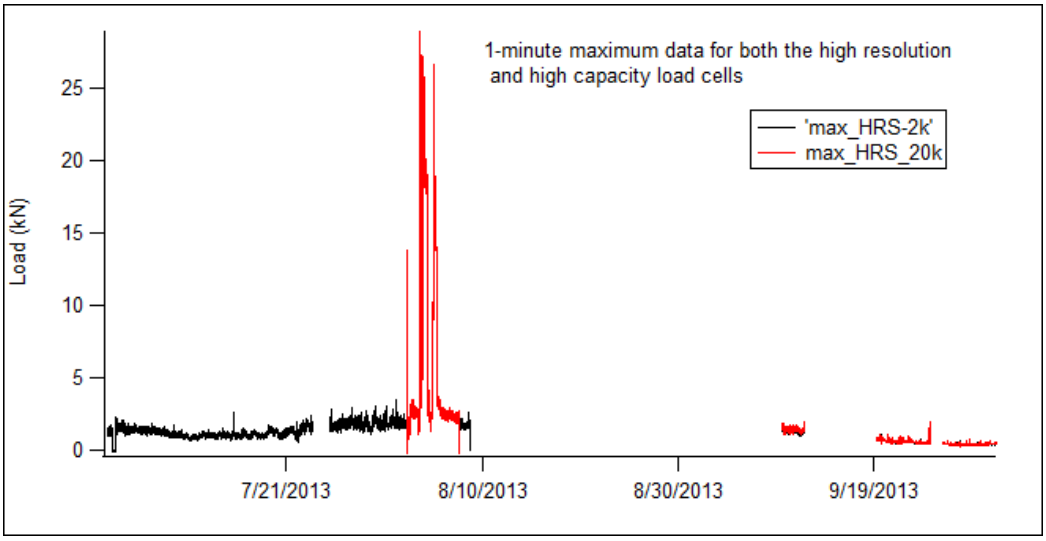

Figure 10. Drag and impact forces acting on the RDDP during 2013.

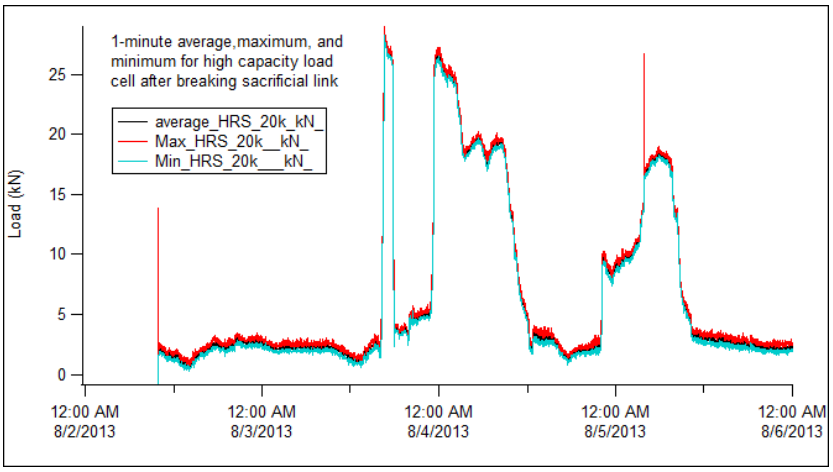

Figure 11. Expanded view of impact forces on the RDDP from August 3–5, 2013.

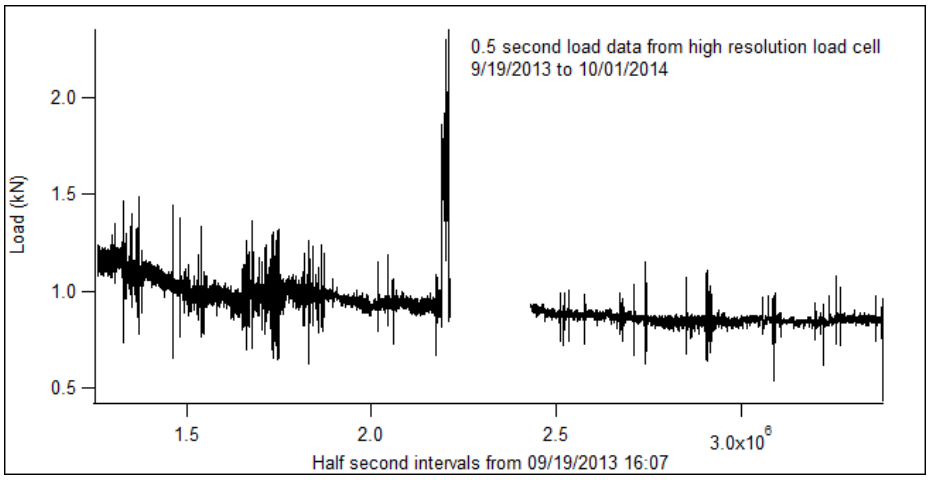

Figure 12. Expanded view of impact forces on the RDDP for September 19, 2013.

The second impact event occurred around midnight on August 4, 2013, with an initially high impact load that gradually decreased, then decreased further to a lower magnitude for several hours before dropping to nearly pre-impact forces. In this case, the debris object may have impacted the RDDP and then gradually changed its orientation, resulting in a reduced load from current flow before finally clearing. The third impact event indicates an initial debris impact just before midnight on August 5, with subsequent debris buildup and a debris impact during early morning (August 5 at 3:49 a.m.), with all debris clearing the RDDP around 10:15 a.m.

Natural debris impacts that produce large forces on the RDDP do not generally clear the platform immediately after impact, in contrast to test debris impacts (e.g., the sharp impact signal from tests conducted shortly after redeploying the RDDP on August 8, Figure 10). Natural debris impacts may not always result in sudden impact and clearing as occurs during debris impact tests or when relatively small impacts occur, such as the one on September 19, 2013 (Figure 12). It may take several hours for large debris to clear the RDDP, as river turbulence and asymmetric torque on the debris sweep help debris slide off the platform.

Indications that the mooring buoy also experienced significant debris impacts during 2013 are that the buoy was significantly dented and that woody fragments were scraped off and wedged in the bunghole on the mooring buoy. Observations indicated that no debris hung up on the mooring buoy during its deployment.

Forces recorded on the load cell sensor during the short September 2014 deployment, along with the U.S. Geological Survey (USGS) river stage, are shown in Figure 13. Loads were due to either river drag action on the RDDP/test barge system or the Oceana turbine, when it was lowered into the water. The load spikes above the background river drag are the result of turbine drag during turbine operations. No debris impacts with the RDDP were observed during the test period. Due to a data logger issue, forces between 5.3 kN (1,200 lbf) and 8.9 kN (2,000 lbf) were not recorded, but as the sacrificial link did not break, no forces in excess of 8.9 kN (2,000 lbf) occurred during this period. The data void from August 21 to September 4 corresponds to a dead battery episode.

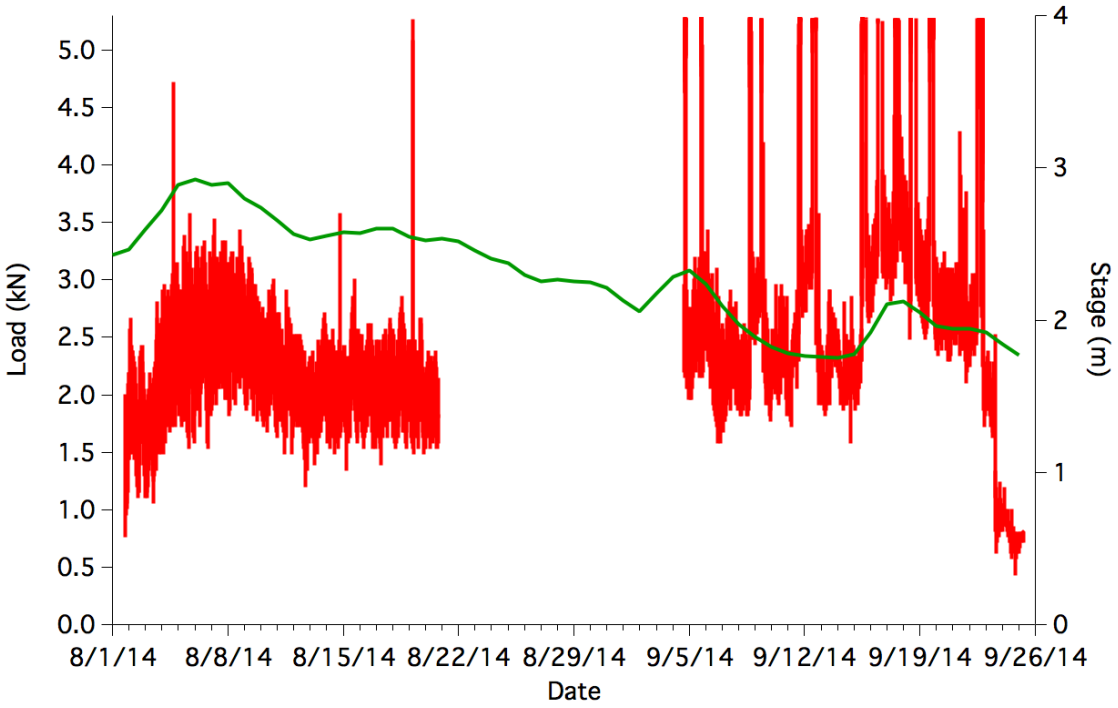

Figure 13. Drag and impact forces acting on RDDP and river stage during 2014.

Hydrodynamic Measurements

Acoustic Doppler current profiler (ADCP) hydrodynamic measurements performed during summer 2013 at the TRTS were first rotated from geographic coordinates into along- and cross-stream coordinates (Dinehart and Burau 2005; Walsh et al. 2012). Velocities from the horizontal plane were then transformed into along-channel and cross-sectional velocities using the calculated angle between flow orientation and north. The vertical velocity component of the axis of rotation is unchanged. After rotation, measurements are projected onto an ideal straight transect. An optimal interpolation scheme is used to interpolate the spatially varying measurements onto a fixed grid. After gridding, average velocity sections can be calculated, as can vorticity and deviations from the average velocity (i.e., the turbulence fluctuations). A set of MATLAB routines was developed to automate this procedure, and a publication describing the gridding procedure is in preparation (Duvoy et al. *in prep*).

To analyze the effect of the RDDP on the mean flow, four transects at each of three distances downstream of the RDDP (6 m, 25 m, and 47 m) from July 3 and 4 were processed. For each location, an ideal transect was computed. The RDDP is located approximately 70 m from the left bank in each transect.

Vorticity (i.e., the rotational tendency, units s^{-1}) and streamwise turbulent fluctuation ($u'^2=(U-u)^2$, where u'^2 is the streamwise fluctuation squared, U is the mean velocity at the grid point, and u is the instantaneous velocity at the grid point; all velocities have units of m

s^{-1}) results indicate that natural variability in the river dominates the signals, with no clear pattern evident in either derived quantity. Figures 14 and 15 show results from the 6 m location.

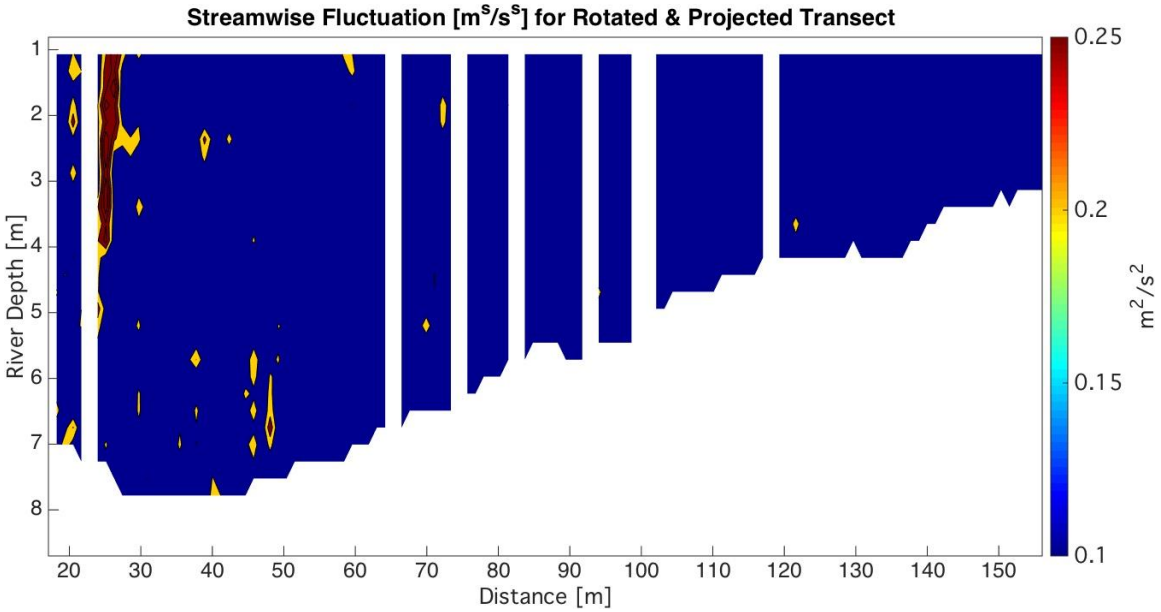

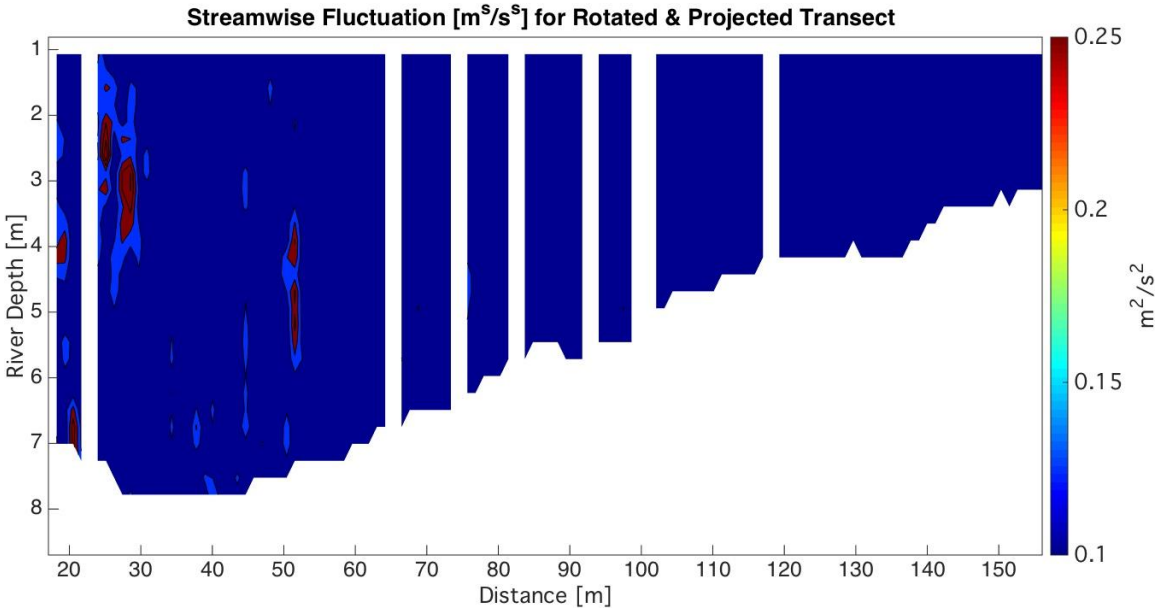

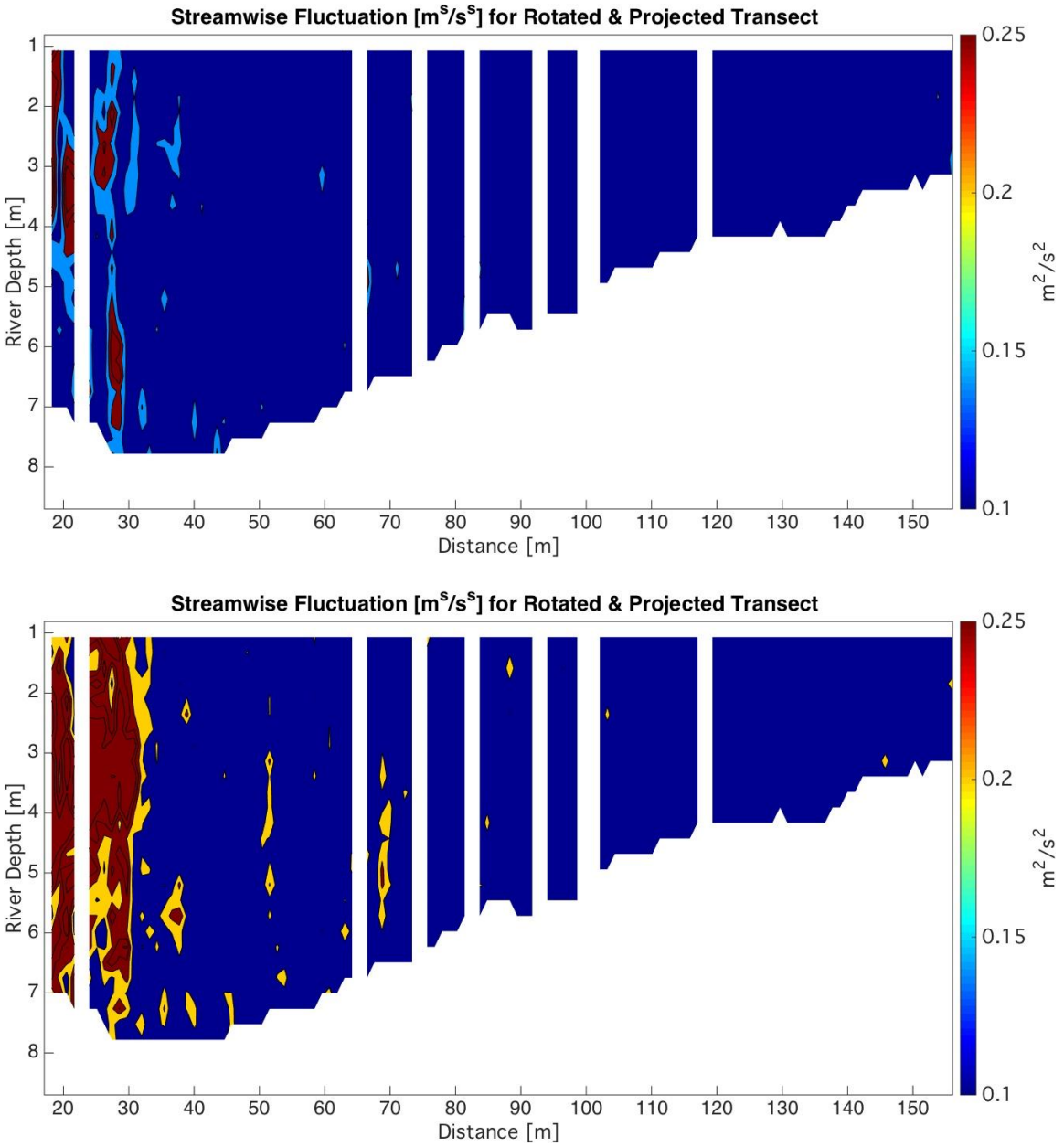

Figure 14. Streamwise fluctuation for each of the four transects from 6 m aft of the RDDP.

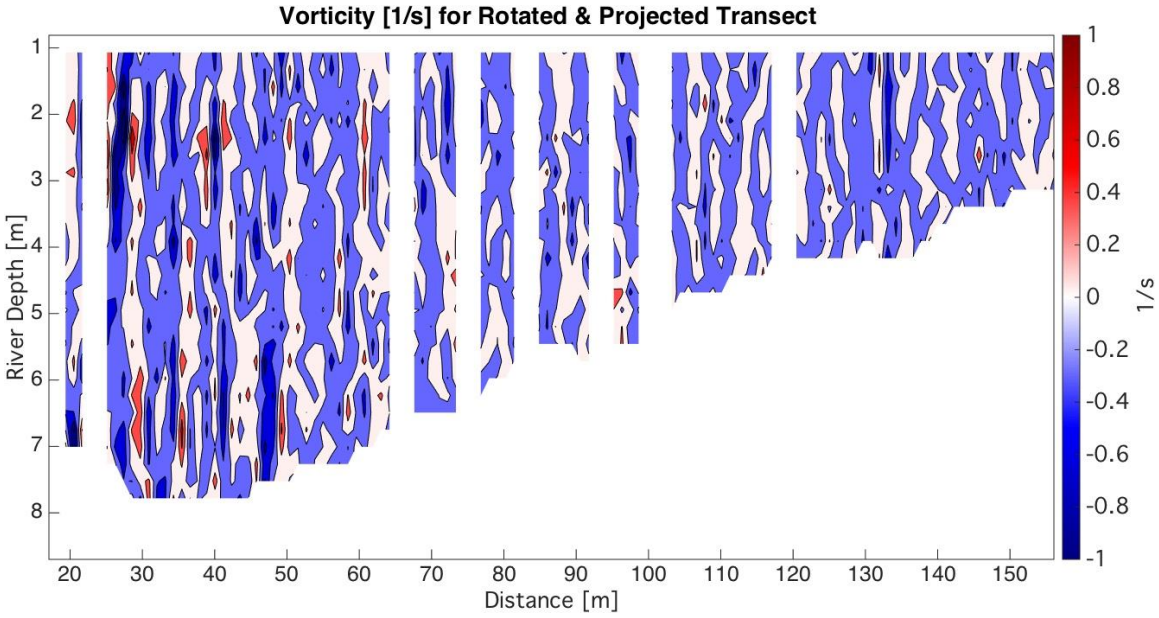
Vorticity [1/s] for Rotated & Projected Transect
River Depth [m]
Distance [m]
1/s

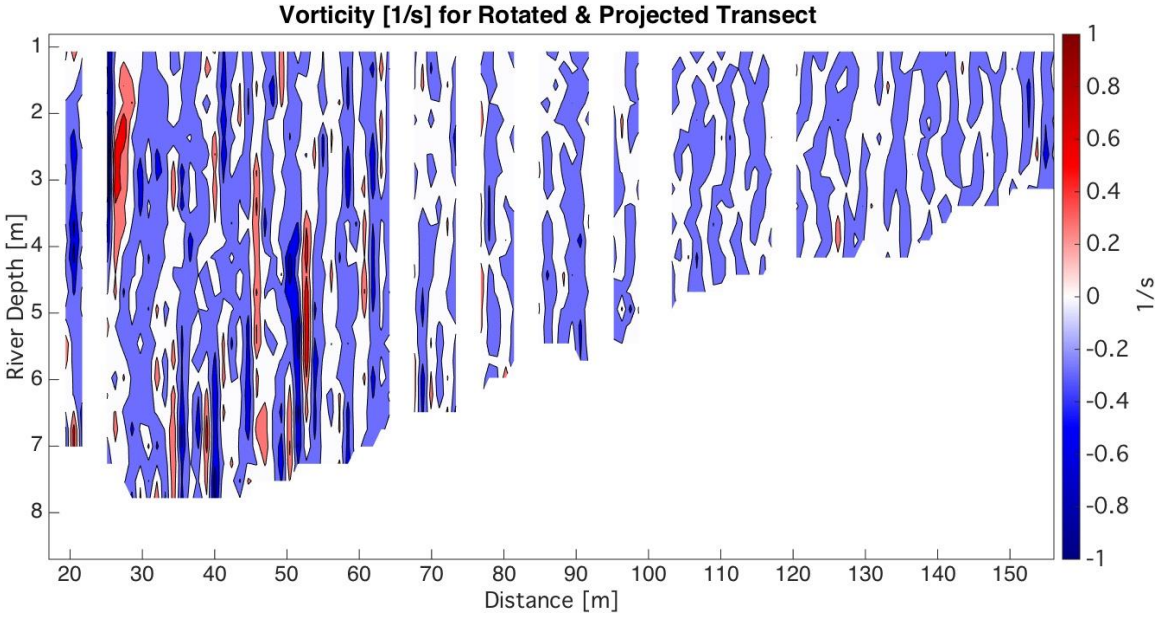
Vorticity [1/s] for Rotated & Projected Transect
River Depth [m]
Distance [m]
1/s

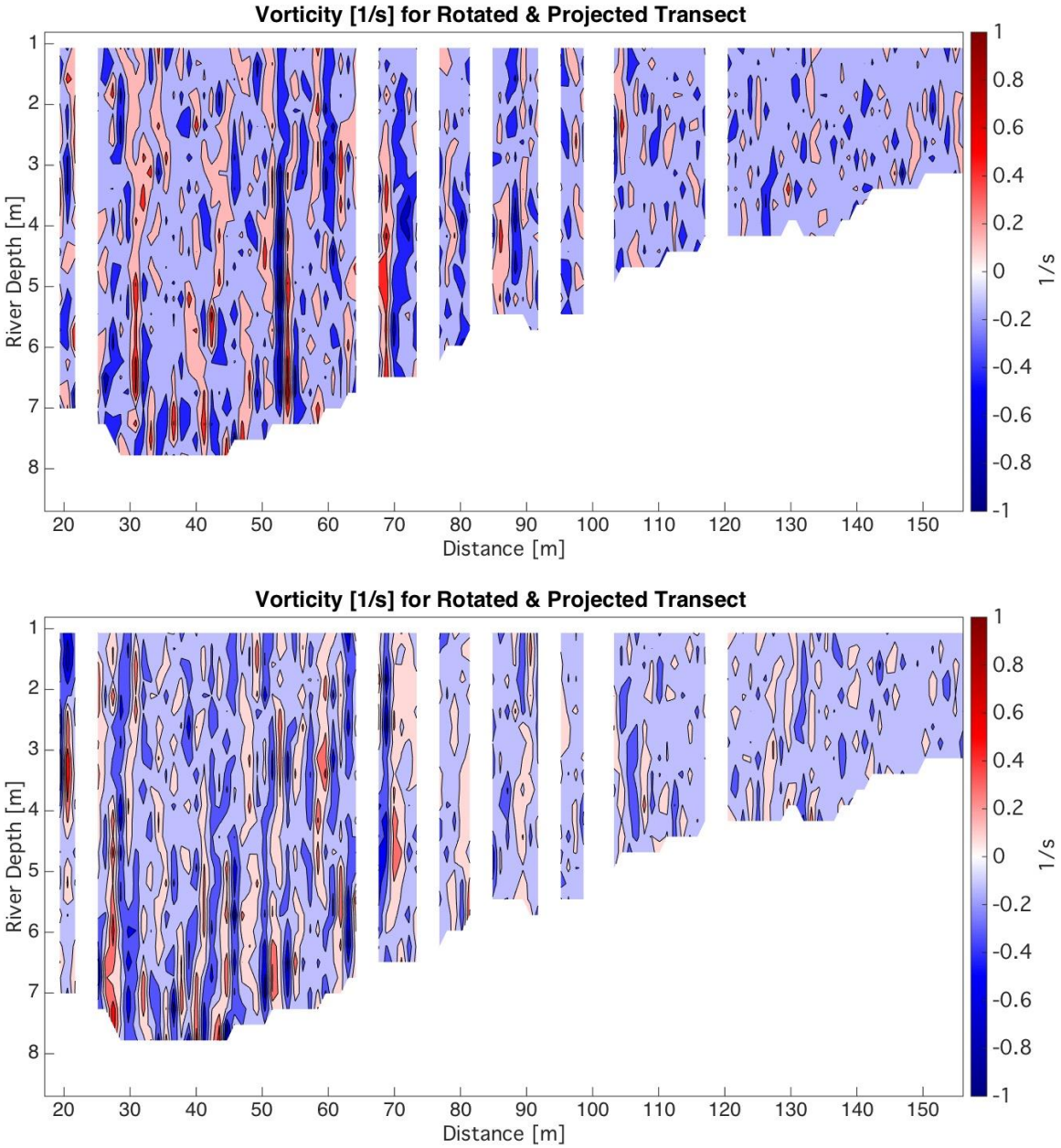

Figure 15. Vorticity for each of the four transects surveyed 6 m aft of the RDDP.

The difference in primary and secondary velocities was also calculated between 6 m aft of the RDDP and 25 m (Figure 16) and 47 m (Figure 17) aft of the RDDP. While the velocities at the three locations are similar, the largest differences are between 6 m and 47 m aft of the RDDP: a small increase in cross-stream velocity occurs near the surface 70 m from the left bank.

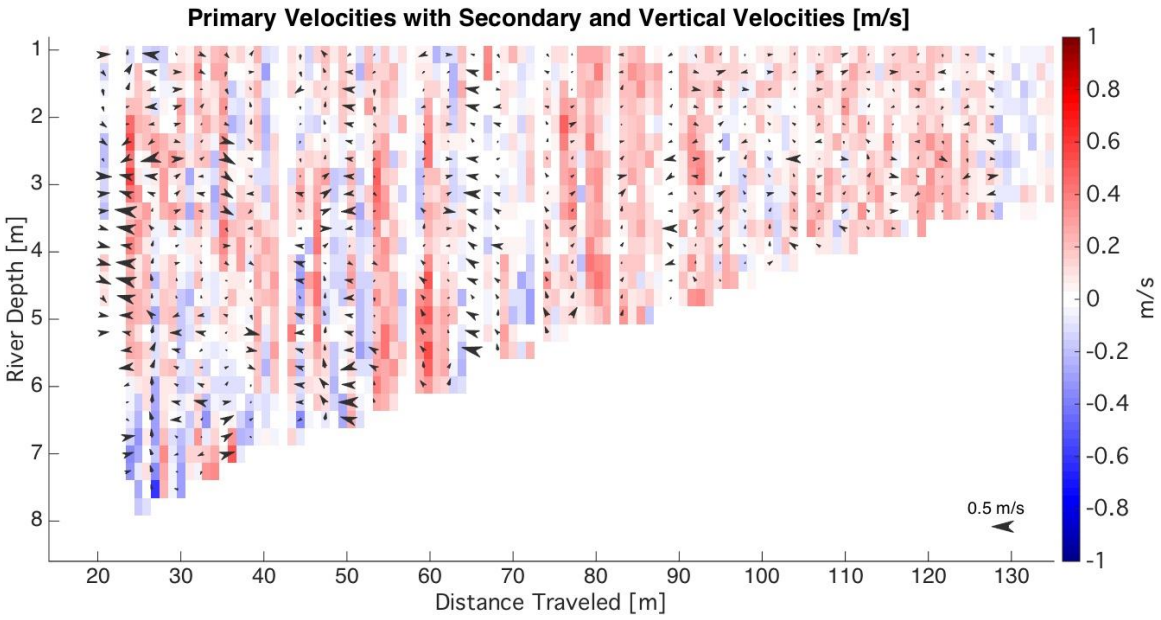

Figure 16. Velocity difference between ideal transects 6 m and 25 m aft of the RDDP.

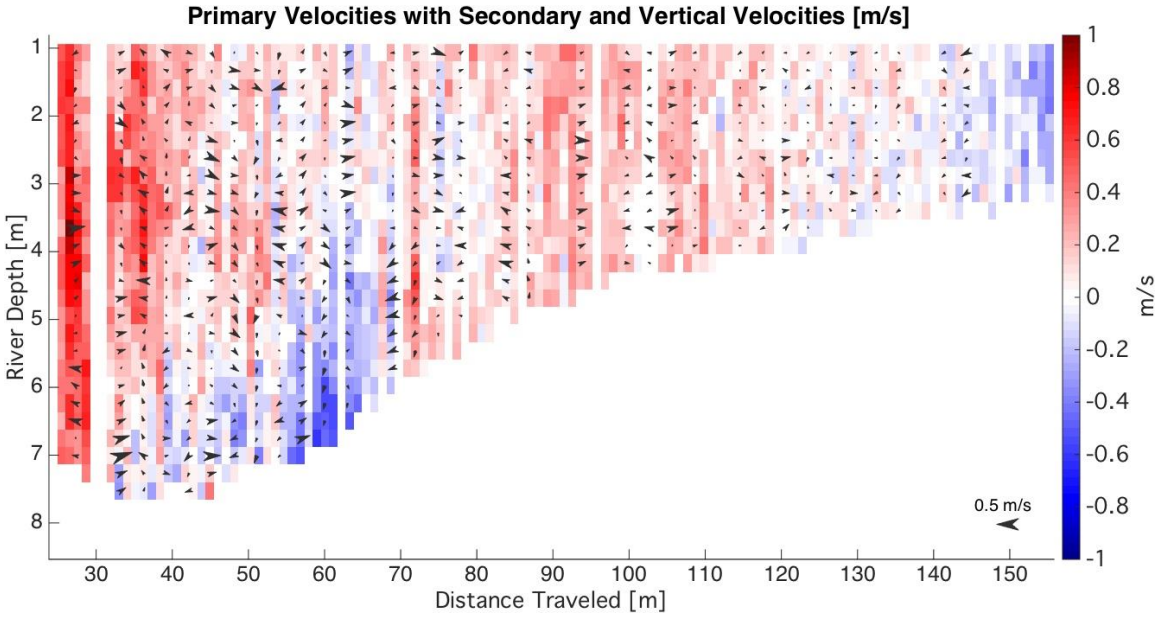

Figure 17. Velocity differences between ideal transects 6 m and 47 m aft the RDDP.

BlueView Sonar Measurements of Subsurface Debris

Our preliminary analysis indicates that using the BlueView to detect subsurface debris and activate a debris diversion system would require a significant investment of time, since the computer algorithms necessary to identify and track debris in the sonar images would need to be written. Thus, we are currently assessing other means of achieving the same result. In addition, through cooperation with the Alaska Department of Fish and Game, AHERC conducted a side-by-side evaluation of the BlueView system and a DIDSON sonar camera to determine if the DIDSON was more suitable for debris identification than the BlueView.

Both systems have the same shortcoming, in that their ability to locate debris with enough lead time to activate any mitigation strategy is limited. The Tanana River, with its high sediment load, attenuates the systems' acoustic signals, leaving a short distance for either system to detect debris. Another shortcoming of the BlueView system is the instability of the vendor-provided software to visualize the data in real time. We are currently working with the vendor to address these issues. In addition, we are exploring alternative sensors and techniques (e.g., mechanical) to detect and characterize subsurface debris. Testing improved versions of the BlueView operating system, comparing the BlueView with mechanical debris detection techniques, and evaluating means of post-processing BlueView data using existing software packages are goals of the ongoing DOE ALFA project. Another goal of the ALFA project is to use a dual sonar system (split beam and BlueView) to understand subsurface debris and its distribution in a manner similar to the VDOS, described in the next section of this report. A secondary goal of BlueView measurements was to determine whether debris data collected using the BlueView system could be co-analyzed for the presence/absence of small salmon smolt during periods when fisheries data are lacking. This determination is in progress.

During summer 2014, at the request of the Alaska Department of Fish and Game, a calibrated 120 kHz scientific echo sounder (a Simrad EK60 split-beam sonar) was deployed for evaluating its utility in tracking fish and debris. Split-beam sonars have been used successfully in the past in Alaska for counting and tracking adult salmonids. AHERC continues its collaboration with the Alaska Department of Fish and Game and researchers at the University of Washington to optimize the collection of sonar data in support of fisheries and debris studies. At the 2014 Global Marine Renewable Energy Conference, AHERC learned that another manufacturer of split-beam sonars, BioSonics, has successfully used a split-beam system similar to UAF's to track debris near nuclear power cooling-water intakes as part of an active "debris warning system."

Video Debris Observation System Observations

Data from the video debris observation system (VDOS) were used to define a debris index: the number of debris items counted in the first 5 minutes of every hour during daylight hours. Debris were categorized by size (large, medium, or small; see Figure 6) and by location in the river channel, referencing the downstream direction (left, middle, right). A debris index by location and size is shown in Figure 18, and a debris index by size for each channel location is shown in Figure 19.

Two important aspects of debris flow in the river are that most debris travels in the left or mid channel part of the river, with little debris on the right side of the river (Figure 18a), and most debris is small to medium in size; there are few large debris items. The amount of debris, of all sizes, increases with river stage in the middle and left channel, and large debris is mobilized with increasing river stage (Figure 18b). One large debris object was mobilized on September 16 (Figure 18b and Figure 6a). In Figure 19, the amount of debris by size is shown for the left, middle, and right river channels. As shown in Figure 18, most debris is carried in the middle channel, with the next highest number of debris objects carried in the left river channel, and the least amount of debris (the scale on the plots in Figure 19 are not the same) carried by the right channel.

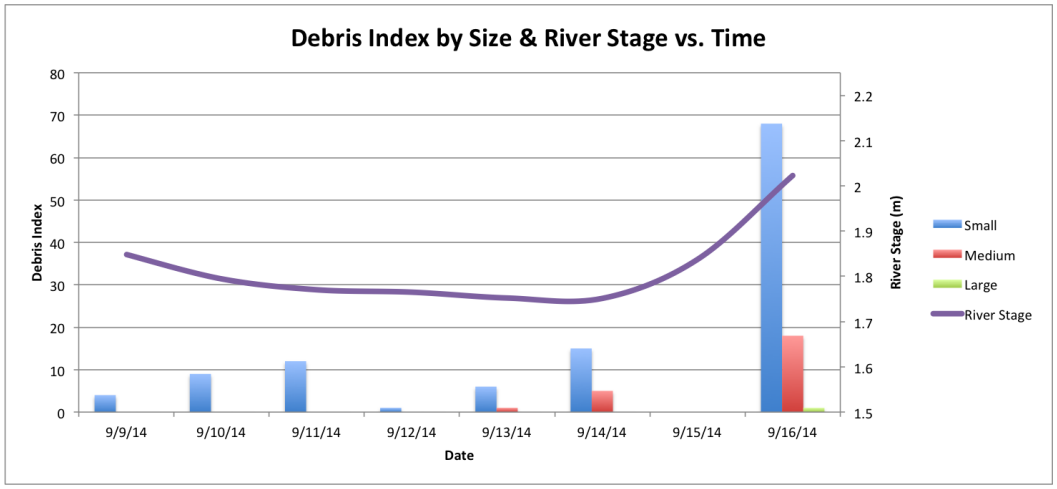

a

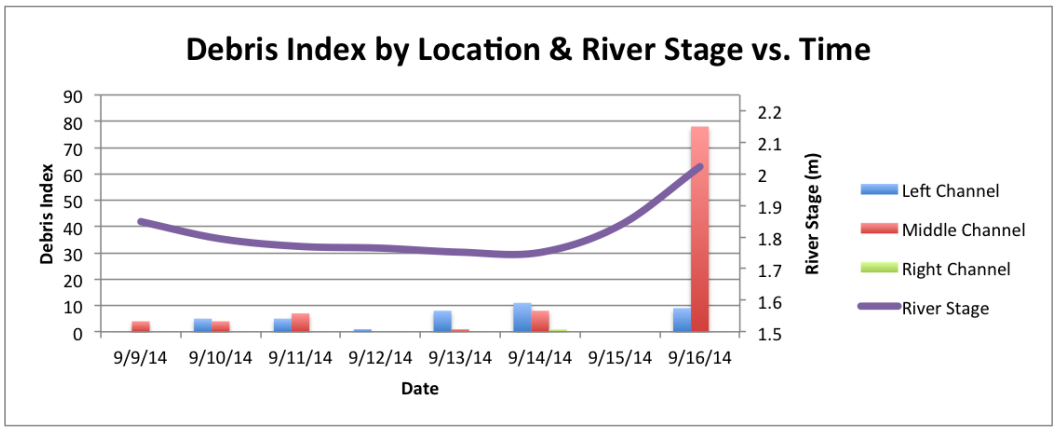

b

Figure 18. Debris index as a function of location in the river (a) and as a function of debris size (b). River stage is also plotted.

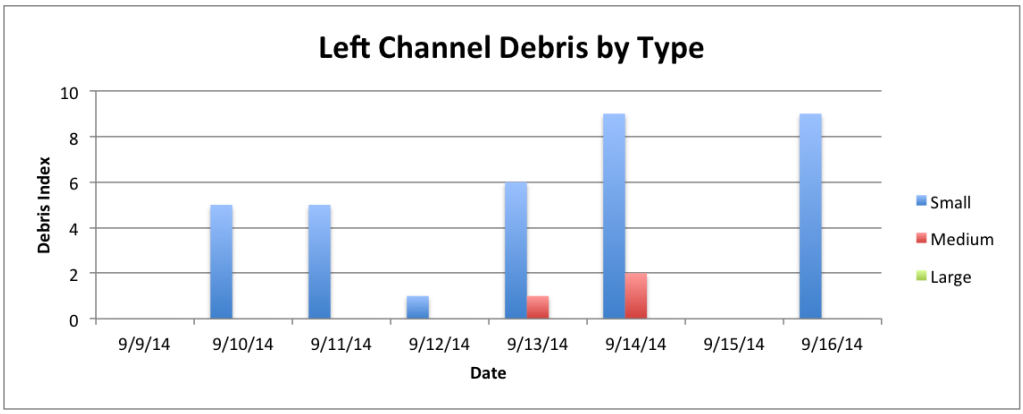

a

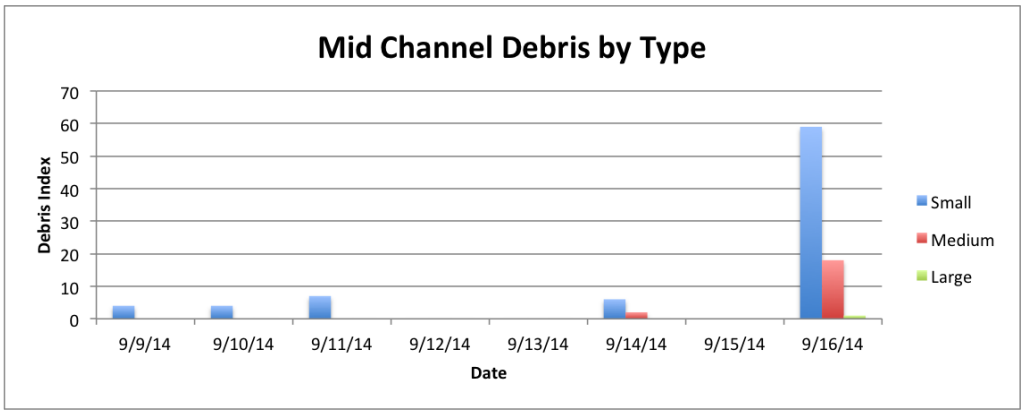

b

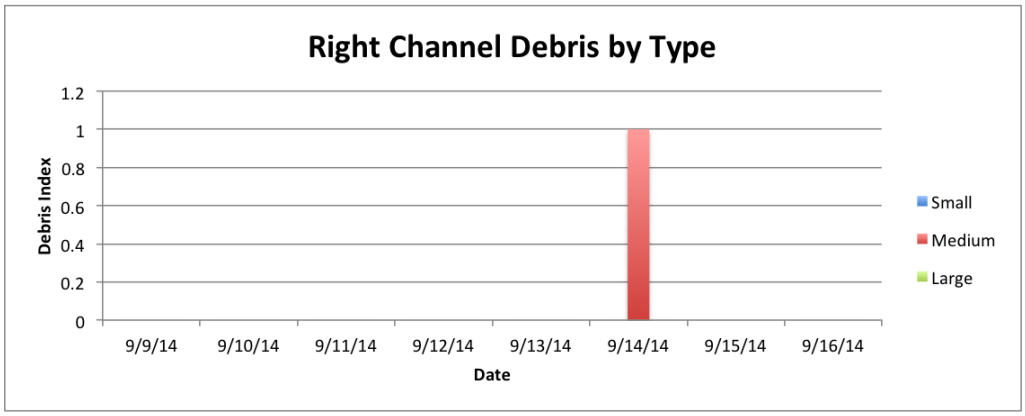

c

Figure 19. Debris index as a function of size for the left channel (a), mid channel (b) and right channel (c).

Discrete Element Method Modeling of Debris Impact on the RDDP

Three debris impact scenarios were simulated by COUPi DEM to examine the interaction behavior of debris with the RDDP debris sweep as a function of contact friction and debris size and geometry. Observations from debris impact tests indicate that debris could become torque-balanced on the debris sweep if friction between the sweep and debris object is

sufficiently high; the DEM simulations support these observations (Figures 20 and 21). In Figure 20, nine stages of the DEM simulation of a debris object impacting the RDDP debris sweep, with a coefficient of friction of 0.5 between the debris object and the debris sweep, are shown (from left to right and top to bottom). Frames 1 and 2 show the debris moving toward the RDDP; Frame 3 shows the debris impacting the debris sweep. The debris object then oscillates about the debris sweep in a torque balance without clearing the RDDP (Frames 4–9). A second DEM simulation of debris impact with the RDDP, resulting in a contact friction coefficient of 0.3, is shown in Figure 21.

In Figure 22, a tree with a root ball impacts the RDDP with a contact friction coefficient of 0.1. The purpose of this simulation was to examine the effect of the protrusions associated with the root ball on the RDDP's ability to divert the debris object. In this simulation, the debris object is diverted by the RDDP using a relatively low friction coefficient compared with the simulation of debris shown in Figures 20 and 21. It is expected that the ability of the debris sweep to shed debris objects that include root balls will depend on the length of the root ball projection, the contact friction, the radius of the debris sweep, and the opening angle of the RDDP pontoons. In Figure 22, Frames 1 and 2 show the debris object moving toward the RDDP. Frame 3 shows the debris object impacting the debris sweep. The debris object then slides off the debris sweep (Frames 4–6) and along the RDDP pontoon surface, and clears the RDDP, showing the importance of reducing the frictional surfaces of the RDDP.

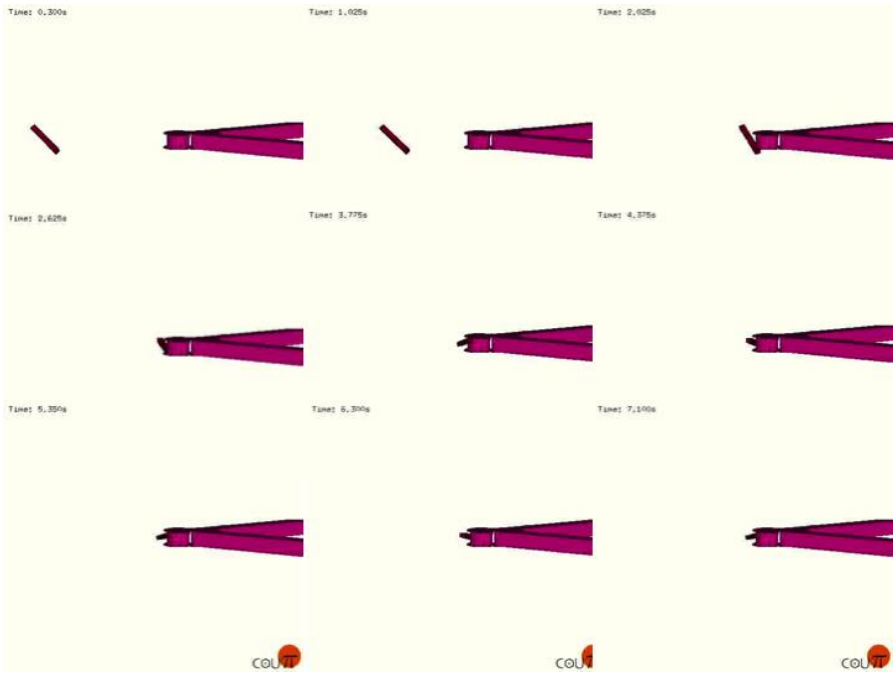

Figure 20. DEM simulation of a log impact on the RDDP with contact friction coefficient equal to 0.5, showing a balanced debris object on the debris sweep. Figure order is from left to right and top to bottom; simulation time is shown.

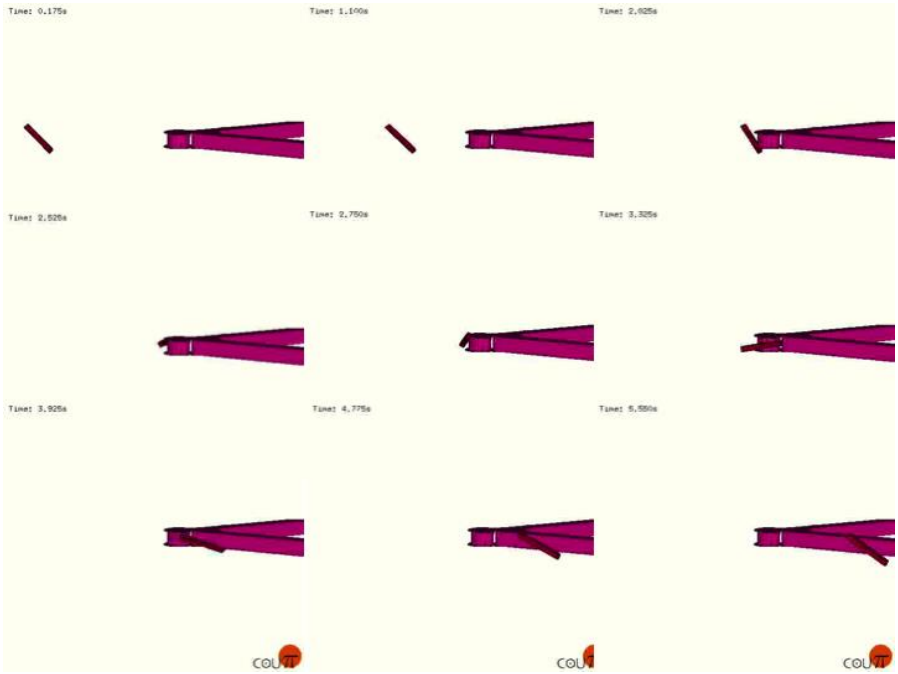

Figure 21. DEM simulation of a log impact on the RDDP with contact friction coefficient equal to 0.3, showing a debris object impact then clear the debris sweep.

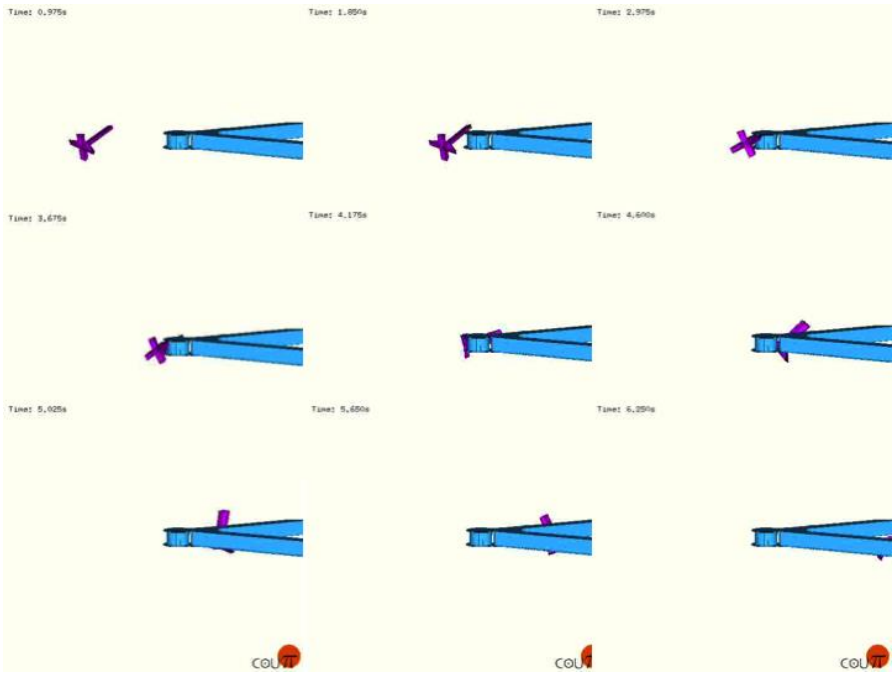

Figure 22. DEM simulation of a log impact on the RDDP with contact friction coefficient equal 0.1, showing a debris object impact then clear the debris sweep.

Oceana Turbine Testing and the Influence of River- and RDDP-Generated Turbulence

Turbulence in the current flow of rivers can cause fluctuations in the power output of hydrokinetic turbines. River turbulence occurs naturally when the flow direction of water changes due to variations in bathymetry, river bends, riverbank projections into the flow, and other sources. Energetic eddies with diameters as large as or larger than the ~2 m diameter turbine are commonly observed at the TRTS (Figure 23a). River turbulence can also be generated by the RDDP due to water upwelling from under the front of the platform, water being diverted around the platform, and vortices forming at the ends of the pontoons (Figure 23b). Natural and RDDP-generated turbulence can reduce mean flow velocity (Birjandi et al. 2012) and a REC's power production.

Performance tests of the Oceana turbine had been conducted at the Navy's Carderock tow tank before the test program on the Tanana River. The Carderock tests demonstrated that the Oceana turbine generated constant power output at a given velocity in low Reynolds number conditions. Oceana turbine tests in the turbulent river at the TRTS produced variable power output (Figure 24).

Power from the Oceana turbine was fed into a load bank. The turbine power output for the three locations downstream from the RDDP is shown in Figure 24. The difference in power at locations of 14.5 and 50 m as compared with the power 100 m downstream of the RDDP is shown in Table 2, where $\bar{V}$ is the mean river current velocity, $\bar{P}$ is the mean power output in Watts, $2\sigma/\bar{P}$ is the percent variation of the power output at two standard deviations about the mean power, and $\Delta\bar{P}/\bar{P}_{100}$ is the percent difference of the mean power output at the 100 m location compared with the power output at the 14.5 m and 50 m locations.

The results shown in Figure 24 and Table 2 indicate that natural turbulence from the river caused Oceana turbine power fluctuations of about 150 W at a downstream distance of 100 m. This is about 1% of the mean power produced by the Oceana turbine at 100 m. The 100 m test location is considered relatively unaffected by RDDP-generated turbulence, because the difference between the Oceana turbine's mean power output at the 50 m and 100 m locations is only -0.3%. Turbulence generated by the RDDP reduced the mean power output of the Oceana turbine by about 8.3% at the 14.5 m test location compared with the 100 m test location.

The effects of turbulence generated by the RDDP drops off to negligible values within 50 m distance downstream. However, it is not practical to place the test turbine that far downstream from the RDDP and have it provide adequate protection for debris. Experience demonstrates that on a river such as the Tanana, where the river channel swings from one river bend to another, the current seldom remains in a parallel flow condition for long and debris sometimes curves around behind the RDDP. The best protection from debris is provided with the barge attached to the RDDP by a bridle, as shown in Figure 9.

Figure 23a. Vortex eddy (~ 3 m) moving downstream toward the RDDP on the Tanana River.

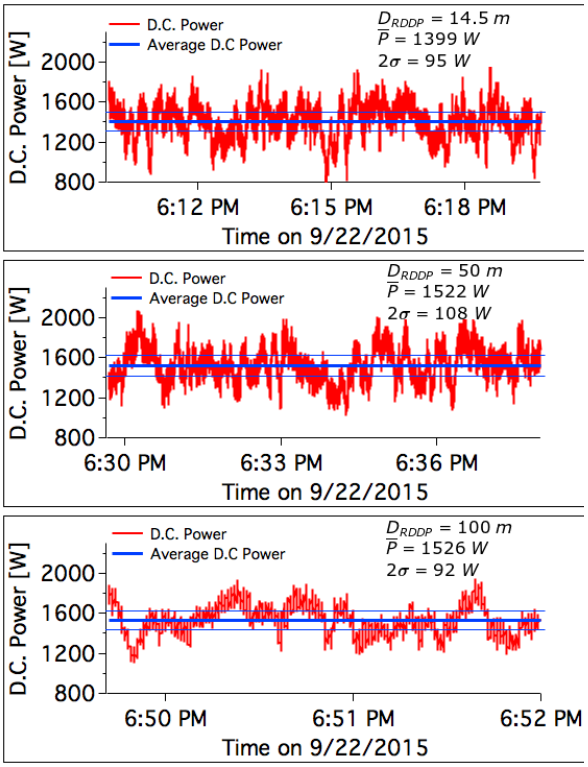

Figure 24. Oceana turbine power output at downstream distances from the RDDP of 14.5 m, 50 m, and 100 m. The variation of two standard deviations about the mean power is shown by thin blue lines on either side of a thicker blue line (mean value).

Figure 23b. Downstream view of RDDP-generated turbulence.

Table 2. Oceana turbine mean power, variation, and power difference from the 100 m downstream location.

D_{RDDP} (m)	$\bar{V}$ (m/s)	$\bar{P}$ (W)	$2\sigma/\bar{P}$ (%)	$\Delta\bar{P}/\bar{P}_{100}$ (%)
14.5	1.65	1399	**6.8**	**-8.3%**
50	1.65	1522	7.1	-0.3%
100	1.65	1526	6.0	-

Results from the Oceana turbine testing show no significant differences in mean current velocities recorded by the ADCP at the three different test locations. This indicates that the differences observed in the power output of the Oceana turbine are the result of factors not captured by the ADCP measurements. Since the ADCP sampled at f~1 Hz, it is only capable of sampling turbulence with frequencies less than 0.5f (0.5 Hz). Using Taylor's frozen turbulence hypothesis and assuming mean velocities, U~O(1.65 m s^{-1}) means the ADCP only accurately samples eddies with wavelengths, $\lambda > 3.30$ m ($\lambda = U/0.5f$). This implies that differences in turbulence wavelength not captured by the ADCP measurements are responsible for the measured differences in the Oceana turbine power output, as the small difference in mean velocity between the two locations cannot account for variation in device power output. Eddies just behind the RDDP are visibly smaller than eddies outside of the RDDP's wake (e.g., Figure 23b). Eddy size far downstream of the RDDP appears to revert to the eddy size distribution characteristic of the undisturbed river.

The ADV unit includes an integrated inertial sensor that was configured to record motion data simultaneously with velocity data. During measurements, the velocity data were heavily contaminated with the motion of the ADV, which could not be completely filtered out with further post-processing. This issue and its solution are being investigated.

Numerical model calculations using the CCHE2D package show no difference in velocity magnitude, specific discharge, or the ratio between average turbulence kinetic energy and turbulence kinetic energy at the three test locations behind the RDDP (Duvoy and Toniolo. 2012). While the CCHE2D results do not account for the presence of the RDDP, the model results indicate that along-stream differences in Oceana turbine power output are not solely caused by naturally occurring variations in river hydrodynamics and that changes in turbulence size due to the presence of the RDDP are likely responsible for the variation in REC power output. Moreover, the differences in mean velocities at different distances behind the RDDP calculated from the ADCP transects and discussed earlier are too small to account for the measured difference in device power output.

Summary

Tests and analyses of debris impacts on the RDDP indicate that its ability to divert and clear debris objects improves significantly when all surfaces that come into contact with debris are covered with a low-friction material, such as high-density plastic. The RDDP profile in the water is improved by proper ballasting to counterbalance the downward drag at the front of the RDDP caused by water displaced under the front of the debris sweep. The RDDP and

mooring buoy system demonstrated the capability of withstanding significant debris impact during their long-term deployment. During August 2014, the RDDP cleared debris after three large-scale impacts of up to 29 kN (6,600 lbf). Some of the debris took more than 6 hours to clear. From interpretation of load cell data, the debris impacts consisted of both single debris objects and multiple debris objects. Additionally, the ability of the RDDP to successfully protect a REC was demonstrated in September 2014, when the RDDP was deployed in front of the Oceana turbine. As of June 2015, the RDDP is deployed in the Tanana River in preparation for the second year of Oceana testing and for UAF testing of a 5 kW New Energy turbine, planned for August 2015.

A method for analyzing cross-river ADCP transects was developed to (1) maximize information derived from such standard, widely used ADCP measurements, and (2) enable the analysis of large-scale turbulence and determine its effects on REC performance. River velocity measurements performed during summer 2013 at the TRTS were rotated into along- and cross-stream directions and projected onto an ideal straight transect. An optimal interpolation procedure was applied by means of MATLAB routines developed for the project that allow irregularly spaced measures to be interpolated onto an equally spaced grid. From these gridded transects, averages and deviations from the average are calculated to characterize turbulence velocity fluctuations. The gridding analysis showed very little influence on the mean flow field (or vorticity) due to the presence of the RDDP, though questions about smaller-scale turbulence remain and require further development of measurement and analysis techniques. Additionally, a short series of ADCP and ADV measurements were made on the last day of the Oceana's deployment in 2014 to determine the influence of the RDDP on REC performance. These measurements demonstrated that power output behind the RDDP is reduced and that the influence of the RDDP decreases with increasing distance from the platform. As no statistically significant difference was found between the mean velocity at hub height at three distances behind the RDDP, we concluded that the reduction in power output is most likely due to the effect of the RDDP on turbulence.

Preliminary investigation of whether a BlueView sonar "camera" is suitable for detecting debris was largely unsuccessful because we were unable to obtain long-term observations with the system. In 2013, BlueView's operating software continually "hung up" when we used the "camera" on multiple day-long deployments. We determined that the AHERC BlueView system is unable to detect debris beyond ~15 m, due to signal scattering by the sediment carried in the Tanana River. In discussions with Teleydyne BlueView, we learned that the company has a lower frequency (450 kHz) sonar that may perform better in the heavily silted Tanana River than higher frequency sonars such as the one AHERC currently possesses. Teledyne BlueView indicated an interest in working with AHERC on the resolution and software reliability issues. The most recent versions of the Teledyne BlueView operating software appear to address past reliability issues, though this remains to be field-tested. A split-beam sonar owned by UAF was deployed in September 2014 for fisheries monitoring in support of the Oceana turbine tests and was repeatedly operated for periods of up to a full day unattended using only a small Honda generator as a power source. With funding from the U.S. Department of Energy, a power and data system has since been developed for long-term operation of the BlueView and split-beam sonar systems.

Significant improvements were made to the video debris observation system (VDOS). The VDOS is now able to record images of the river and floating debris at one frame per second, both from shore and from the RDDP. The imagery is then used to determine the size, location, and amount of surface debris in the river and to observe the interaction between debris and the RDDP. The VDOS was first built and tested in a breadboard configuration (i.e., a lab setting), and subsequently, a long-term performance test at the Tanana River test site was completed, in conjunction with the Oceana turbine deployment. Presently, the VDOS is capable of long-term autonomous operation and thus is a suitable tool for use in remote locations where hydrokinetic projects are being considered.

The capability and techniques for simulating debris interactions with hydrokinetic infrastructure such as the RDDP were developed. We used the COUPi DEM to simulate the impact of debris on the RDDP, providing a qualitative way to examine the process of debris interaction with the platform and the debris sweep. Simulations indicate that the ability of the RDDP to clear debris is influenced by the contact friction between debris and the RDDP as well as the shape of the debris object. With funding from the U.S. DOE ALFA project, the COUPi DEM simulations will be improved by adding the effects of buoyancy and more realistic RDDP features including a rotating debris sweep and a variable opening angle between the RDDP pontoons.

Conclusions

The research debris diversion platform (RDDP) and buoy system, developed during prior work directed by Alaska Power and Telephone and refined under this project, has proven a robust platform for protecting surface-mounted river energy converters (RECs) from floating debris. Despite progress, many questions remain about subsurface debris including its potential for disrupting subsurface RECs. The question of how best to bring hydrokinetic power to shore in river waters carrying heavy loads of woody debris remains largely unexplored. While we have made substantial progress in maximizing the utility of acoustic Doppler converter profilers (ADCPs) for making hydrodynamic measurements relevant to REC installations, shortcomings in the current generation of acoustic Doppler velocimeter (ADV) mounts require a greater investment of time to understand smaller-scale turbulence and its effect on REC power output. While the RDDP/buoy/pontoon barge debris protection scheme has proven successful at debris diversion, cost-effective nonresearch installations of RECs in remote communities will require refinements in any REC+debris protection system to achieve affordable and practical implementations. As steps are taken toward employing hydrokinetic energy systems in Alaska's waterways, we must consider the effects of any new hydrokinetic infrastructure on habitat including the impact on fisheries. Finally, given the short open-water season in Alaska, an understanding of the economics of hydrokinetic energy must be determined, including a realistic projection for the levelized cost of energy for hydrokinetic energy systems. Remaining issues require systematic development of new platforms (e.g., improved ADV mounts or simpler, lighter, and stronger debris mitigation schemes integral to REC systems) and techniques (e.g., improved understanding of the limits of sonar for fisheries monitoring in turbid rivers that carry large amounts of woody debris). Such efforts will require the continued cooperation of state and federal agencies, the university, and the private sector.

Acknowledgments

This work was supported by the Alaska Energy Authority grant ADN #R1416 "Debris Characterization and Mitigation."

We thank the City of Nenana, the Nenana Tribal Council, Jason Mayrand, Victor Lord, Robin Campbell, Inland Barge Service, Charlie Hnilicka, Ruby Marine Inc., Matt Sweetsir, Crowley Marine Services, Endil Moore, and Jon's Machine Shop, without whose cooperation and creativity this work would not have been possible.

References

Birjandi, A. H., J. Woods, and E. L. Bibeau (2012). "Investigation of macro-turbulent flow structures interaction with a vertical hydrokinetic river turbine." *Renewable Energy,* 48: 183–192, DOI: 10.1016/j.renene.2012.04.045.

Cundall, P. A., and O. D. L. Strack (1979). "A discrete numerical model for granular assemblies." *Geotechnique*, 29(1): 47–65.

Dinehart, R., and J. Burau (2005) "Averaged indicators of secondary flow in repeated acoustic Doppler current profiler crossings of bends." *Water Resour. Res*., 41, W09405.

Duvoy, P., and H. Toniolo (2012). "HYDROKAL: A module for in-stream hydrokinetic resource assessment." *Computers and Geosciences,* 39: 11, DOI: 10.1016/j.cageo.2011.06.016.

Duvoy, P. X., J. L. Kasper, and J. B. Johnson (in prep). A Gridding Procedure for the Processing of ADCP Velocity Measurements in River Characterizations.

Hopkins, M. A. (2004). "Discrete element modeling with dilated particles." *Journal of Engineering Computations*, 21: 422–430.

Johnson, J. B., and D. M. Pride (2010). River, Tidal, and Ocean Current Hydrokinetic Energy Technologies: Status and Future Opportunities in Alaska. Alaska Center for Energy and Power, Fairbanks, AK, 32 pp.
http://www.uaf.edu/files/acep/2010_11_1_State_of_the_Art_Hydrokinetic_Final.pdf

Johnson, J. B., J. L. Kasper, N. Hansen, P. X. Duvoy, and J. Schmid (2015). The Effects Of River And Debris Diversion Structure Generated Turbulence On The Oceana River Energy Converter. Proceedings of the 3rd Marine Energy Technology Symposium METS.

Johnson, J. B., J. Schmid, J. L. Kasper, A. C. Seitz, and P. Duvoy (2014). Protection of In-river Hydrokinetic Power-Generating Devices for Surface Debris in Alaskan Rivers. University of Alaska Fairbanks, Fairbanks, AK, 61 pp.
http://acep.uaf.edu/media/127881/2014_10_20_Eagle_APT_Final.pdf

Johnson, J. B., H. Toniolo, A. C. Seitz, J. Schmid, and P. Duvoy (2013). Characterization of the Tanana River at Nenana, Alaska, to Determine the Important Factors Affecting Site

Selection, Deployment, and Operation of Hydrokinetic Devices to Generate Power. Alaska Center for Energy and Power, Alaska Hydrokinetic Energy Research Center, Fairbanks, AK, 130 pp., http://www.uaf.edu/files/acep/2013_8_8_HKD_report_with_appendices.pdf

NUL (Northland Utilities Limited) (2012). Information Request, NTPC GRA 2012/13 and 2013/14: 11–13.
http://www.ntpc.com/documents/NTPC%202012_14%20IR%20Response%20-%20NUL,%20June%208,%202012.pdf

Tyler, R. N. (2011). River Debris: Causes, Impacts, and Mitigation Techniques. Alaska Center for Energy and Power, Fairbanks, AK, 33 pp.
http://www.uaf.edu/files/acep/2011_4_13_AHERC-River-Debris-Report.pdf

Walsh, C., J. Fochesatto, and H. Toniolo (2012). The importance of flow and turbulence characteristics for hydrokinetic energy development on the Tanana River at Nenana, Alaska, Proceedings of the Institution of Mechanical Engineers, Part A, *Journal of Power and Energy*, 226: 283–299.